

Measurement of the WW+WZ Production Cross Section Using the Lepton + Jets Final State at CDF II

- T. Aaltonen,²⁴ J. Adelman,¹⁴ B. Álvarez González^{v, 12} S. Amerio^{dd, 44} D. Amidei,³⁵ A. Anastassov,³⁹ A. Annovi,²⁰ J. Antos,¹⁵ G. Apolinari,¹⁸ A. Apresyan,⁴⁹ T. Arisawa,⁵⁸ A. Artikov,¹⁶ J. Asaadi,⁵⁴ W. Ashmanskas,¹⁸ A. Attal,⁴ A. Aurisano,⁵⁴ F. Azfar,⁴³ W. Badgett,¹⁸ A. Barbaro-Galtieri,²⁹ V.E. Barnes,⁴⁹ B.A. Barnett,²⁶ P. Barria^{ff, 47} P. Bartos,¹⁵ G. Bauer,³³ P.-H. Beauchemin,³⁴ F. Bedeschi,⁴⁷ D. Beecher,³¹ S. Behari,²⁶ G. Bellettini^{ee, 47} J. Bellinger,⁶⁰ D. Benjamin,¹⁷ A. Beretvas,¹⁸ A. Bhatti,⁵¹ M. Binkley,¹⁸ D. Bisello^{dd, 44} I. Bizjak^{jj, 31} R.E. Blair,² C. Blocker,⁷ B. Blumenfeld,²⁶ A. Bocci,¹⁷ A. Bodek,⁵⁰ V. Boisvert,⁵⁰ D. Bortoletto,⁴⁹ J. Boudreau,⁴⁸ A. Boveia,¹¹ B. Brau^{a, 11} A. Bridgeman,²⁵ L. Brigliadori^{cc, 6} C. Bromberg,³⁶ E. Brubaker,¹⁴ J. Budagov,¹⁶ H.S. Budd,⁵⁰ S. Budd,²⁵ K. Burkett,¹⁸ G. Busetto^{dd, 44} P. Bussey,²² A. Buzatu,³⁴ K. L. Byrum,² S. Cabrera^{x, 17} C. Calancha,³² S. Camarda,⁴ M. Campanelli,³¹ M. Campbell,³⁵ F. Canelli^{14, 18} A. Canepa,⁴⁶ B. Carls,²⁵ D. Carlsmith,⁶⁰ R. Carosi,⁴⁷ S. Carrillo^{n, 19} S. Carron,¹⁸ B. Casal,¹² M. Casarsa,¹⁸ A. Castro^{cc, 6} P. Catastini^{ff, 47} D. Cauz,⁵⁵ V. Cavaliere^{ff, 47} M. Cavalli-Sforza,⁴ A. Cerri,²⁹ L. Cerrito^{q, 31} S.H. Chang,²⁸ Y.C. Chen,¹ M. Chertok,⁸ G. Chiarelli,⁴⁷ G. Chlachidze,¹⁸ F. Chlebana,¹⁸ K. Cho,²⁸ D. Chokheli,¹⁶ J.P. Chou,²³ K. Chung^{o, 18} W.H. Chung,⁶⁰ Y.S. Chung,⁵⁰ T. Chwalek,²⁷ C.I. Ciobanu,⁴⁵ M.A. Ciocci^{ff, 47} A. Clark,²¹ D. Clark,⁷ G. Compostella,⁴⁴ M.E. Convery,¹⁸ J. Conway,⁸ M. Corbo,⁴⁵ M. Cordelli,²⁰ C.A. Cox,⁸ D.J. Cox,⁸ F. Crescioli^{ee, 47} C. Cuena Almenar,⁶¹ J. Cuevas^{v, 12} R. Culbertson,¹⁸ J.C. Cully,³⁵ D. Dagenhart,¹⁸ M. Datta,¹⁸ T. Davies,²² P. de Barbaro,⁵⁰ S. De Cecco,⁵² A. Deisher,²⁹ G. De Lorenzo,⁴ M. Dell'Orso^{ee, 47} C. Deluca,⁴ L. Demortier,⁵¹ J. Deng^{f, 17} M. Deninno,⁶ M. d'Errico^{dd, 44} A. Di Canto^{ee, 47} G.P. di Giovanni,⁴⁵ B. Di Ruzza,⁴⁷ J.R. Dittmann,⁵ M. D'Onofrio,⁴ S. Donati^{ee, 47} P. Dong,¹⁸ T. Dorigo,⁴⁴ S. Dube,⁵³ K. Ebina,⁵⁸ A. Elagin,⁵⁴ R. Erbacher,⁸ D. Errede,²⁵ S. Errede,²⁵ N. Ershaidat^{bb, 45} R. Eusebi,⁵⁴ H.C. Fang,²⁹ S. Farrington,⁴³ W.T. Fedorko,¹⁴ R.G. Feild,⁶¹ M. Feindt,²⁷ J.P. Fernandez,³² C. Ferrazza^{gg, 47} R. Field,¹⁹ G. Flanagan^{s, 49} R. Forrest,⁸ M.J. Frank,⁵ M. Franklin,²³ J.C. Freeman,¹⁸ I. Furic,¹⁹ M. Gallinaro,⁵¹ J. Galyardt,¹³ F. Garberson,¹¹ J.E. Garcia,²¹ A.F. Garfinkel,⁴⁹ P. Garosi^{ff, 47} H. Gerberich,²⁵ D. Gerdes,³⁵ A. Gessler,²⁷ S. Giagu^{hh, 52} V. Giakoumopoulou,³ P. Giannetti,⁴⁷ K. Gibson,⁴⁸ J.L. Gimmell,⁵⁰ C.M. Ginsburg,¹⁸ N. Giokaris,³ M. Giordani^{ii, 55} P. Giromini,²⁰ M. Giunta,⁴⁷ G. Giurgiu,²⁶ V. Glagolev,¹⁶ D. Glenzinski,¹⁸ M. Gold,³⁸ N. Goldschmidt,¹⁹ A. Golossanov,¹⁸ G. Gomez,¹² G. Gomez-Ceballos,³³ M. Goncharov,³³ O. González,³² I. Gorelov,³⁸ A.T. Goshaw,¹⁷ K. Goulianatos,⁵¹ A. Gresele^{dd, 44} S. Grinstein,⁴ C. Grossi-Pilcher,¹⁴ R.C. Group,¹⁸ U. Grundler,²⁵ J. Guimaraes da Costa,²³ Z. Gunay-Unalan,³⁶ C. Haber,²⁹ S.R. Hahn,¹⁸ E. Halkiadakis,⁵³ B.-Y. Han,⁵⁰ J.Y. Han,⁵⁰ F. Happacher,²⁰ K. Hara,⁵⁶ D. Hare,⁵³ M. Hare,⁵⁷ R.F. Harr,⁵⁹ M. Hartz,⁴⁸ K. Hatakeyama,⁵ C. Hays,⁴³ M. Heck,²⁷ J. Heinrich,⁴⁶ M. Herndon,⁶⁰ J. Heuser,²⁷ S. Hewamanage,⁵ D. Hidas,⁵³ C.S. Hill^{c, 11} D. Hirschbuehl,²⁷ A. Hocker,¹⁸ S. Hou,¹ M. Houlden,³⁰ S.-C. Hsu,²⁹ R.E. Hughes,⁴⁰ M. Hurwitz,¹⁴ U. Husemann,⁶¹ M. Hussein,³⁶ J. Huston,³⁶ J. Incandela,¹¹ G. Introzzi,⁴⁷ M. Iori^{hh, 52} A. Ivanov^{p, 8} E. James,¹⁸ D. Jang,¹³ B. Jayatilaka,¹⁷ E.J. Jeon,²⁸ M.K. Jha,⁶ S. Jindariani,¹⁸ W. Johnson,⁸ M. Jones,⁴⁹ K.K. Joo,²⁸ S.Y. Jun,¹³ J.E. Jung,²⁸ T.R. Junk,¹⁸ T. Kamon,⁵⁴ D. Kar,¹⁹ P.E. Karchin,⁵⁹ Y. Kato^{m, 42} R. Kephart,¹⁸ W. Ketchum,¹⁴ J. Keung,⁴⁶ V. Khotilovich,⁵⁴ B. Kilminster,¹⁸ D.H. Kim,²⁸ H.S. Kim,²⁸ H.W. Kim,²⁸ J.E. Kim,²⁸ M.J. Kim,²⁰ S.B. Kim,²⁸ S.H. Kim,⁵⁶ Y.K. Kim,¹⁴ N. Kimura,⁵⁸ L. Kirsch,⁷ S. Klimenko,¹⁹ K. Kondo,⁵⁸ D.J. Kong,²⁸ J. Konigsberg,¹⁹ A. Korytov,¹⁹ A.V. Kotwal,¹⁷ M. Kreps,²⁷ J. Kroll,⁴⁶ D. Krop,¹⁴ N. Krumnack,⁵ M. Kruse,¹⁷ V. Krutelyov,¹¹ T. Kuhr,²⁷ N.P. Kulkarni,⁵⁹ M. Kurata,⁵⁶ S. Kwang,¹⁴ A.T. Laasanen,⁴⁹ S. Lami,⁴⁷ S. Lammel,¹⁸ M. Lancaster,³¹ R.L. Lander,⁸ K. Lannon^{u, 40} A. Lath,⁵³ G. Latino^{ff, 47} I. Lazzizzera^{dd, 44} T. LeCompte,² E. Lee,⁵⁴ H.S. Lee,¹⁴ J.S. Lee,²⁸ S.W. Lee^{w, 54} S. Leone,⁴⁷ J.D. Lewis,¹⁸ C.-J. Lin,²⁹ J. Linacre,⁴³ M. Lindgren,¹⁸ E. Lipelis,⁴⁶ A. Lister,²¹ D.O. Litvintsev,¹⁸ C. Liu,⁴⁸ T. Liu,¹⁸ N.S. Lockyer,⁴⁶ A. Loginov,⁶¹ L. Lovas,¹⁵ D. Lucchesi^{dd, 44} J. Lueck,²⁷ P. Lujan,²⁹ P. Lukens,¹⁸ G. Lungu,⁵¹ J. Lys,²⁹ R. Lysak,¹⁵ D. MacQueen,³⁴ R. Madrak,¹⁸ K. Maeshima,¹⁸ K. Makhoul,³³ P. Maksimovic,²⁶ S. Malde,⁴³ S. Malik,³¹ G. Manca^{e, 30} A. Manousakis-Katsikakis,³ F. Margaroli,⁴⁹ C. Marino,²⁷ C.P. Marino,²⁵ A. Martin,⁶¹ V. Martin^{k, 22} M. Martínez,⁴ R. Martínez-Ballarín,³² P. Mastrandrea,⁵² M. Mathis,²⁶ M.E. Mattson,⁵⁹ P. Mazzanti,⁶ K.S. McFarland,⁵⁰ P. McIntyre,⁵⁴ R. McNulty^{j, 30} A. Mehta,³⁰ P. Mehtala,²⁴ A. Menzione,⁴⁷ C. Mesropian,⁵¹ T. Miao,¹⁸ D. Mietlicki,³⁵ N. Miladinovic,⁷ R. Miller,³⁶ C. Mills,²³ M. Milnik,²⁷ A. Mitra,¹ G. Mitselmakher,¹⁹ H. Miyake,⁵⁶ S. Moed,²³ N. Moggi,⁶ M.N. Mondragon^{n, 18} C.S. Moon,²⁸ R. Moore,¹⁸ M.J. Morello,⁴⁷ J. Morlock,²⁷ P. Movilla Fernandez,¹⁸ J. Mülmenstädt,²⁹ A. Mukherjee,¹⁸ Th. Muller,²⁷ P. Murat,¹⁸ M. Mussini^{cc, 6} J. Nachtman^{o, 18} Y. Nagai,⁵⁶ J. Naganoma,⁵⁶ K. Nakamura,⁵⁶ I. Nakano,⁴¹ A. Napier,⁵⁷ J. Nett,⁶⁰

C. Neu^z,⁴⁶ M.S. Neubauer,²⁵ S. Neubauer,²⁷ J. Nielsen^g,²⁹ L. Nodulman,² M. Norman,¹⁰ O. Norniella,²⁵ E. Nurse,³¹ L. Oakes,⁴³ S.H. Oh,¹⁷ Y.D. Oh,²⁸ I. Oksuzian,¹⁹ T. Okusawa,⁴² R. Orava,²⁴ K. Osterberg,²⁴ S. Pagan Griso^{dd},⁴⁴ C. Pagliarone,⁵⁵ E. Palencia,¹⁸ V. Papadimitriou,¹⁸ A. Papaikonomou,²⁷ A.A. Paramanov,² B. Parks,⁴⁰ S. Pashapour,³⁴ J. Patrick,¹⁸ G. Paulettaⁱⁱ,⁵⁵ M. Paulini,¹³ C. Paus,³³ T. Peiffer,²⁷ D.E. Pellett,⁸ A. Penzo,⁵⁵ T.J. Phillips,¹⁷ G. Piacentino,⁴⁷ E. Pianori,⁴⁶ L. Pinera,¹⁹ K. Pitts,²⁵ C. Plager,⁹ L. Pondrom,⁶⁰ K. Potamianos,⁴⁹ O. Poukhov*,¹⁶ F. Prokoshin^y,¹⁶ A. Pronko,¹⁸ F. Ptchosⁱ,¹⁸ E. Pueschel,¹³ G. Punzi^{ee},⁴⁷ J. Pursley,⁶⁰ J. Rademacker^c,⁴³ A. Rahaman,⁴⁸ V. Ramakrishnan,⁶⁰ N. Ranjan,⁴⁹ I. Redondo,³² P. Renton,⁴³ M. Renz,²⁷ M. Rescigno,⁵² S. Richter,²⁷ F. Rimondi^{cc},⁶ L. Ristori,⁴⁷ A. Robson,²² T. Rodrigo,¹² T. Rodriguez,⁴⁶ E. Rogers,²⁵ S. Rolli,⁵⁷ R. Roser,¹⁸ M. Rossi,⁵⁵ R. Rossin,¹¹ P. Roy,³⁴ A. Ruiz,¹² J. Russ,¹³ V. Rusu,¹⁸ B. Rutherford,¹⁸ H. Saarikko,²⁴ A. Safonov,⁵⁴ W.K. Sakumoto,⁵⁰ L. Santiⁱⁱ,⁵⁵ L. Sartori,⁴⁷ K. Sato,⁵⁶ A. Savoy-Navarro,⁴⁵ P. Schlabach,¹⁸ A. Schmidt,²⁷ E.E. Schmidt,¹⁸ M.A. Schmidt,¹⁴ M.P. Schmidt*,⁶¹ M. Schmitt,³⁹ T. Schwarz,⁸ L. Scodellaro,¹² A. Scribano^{ff},⁴⁷ F. Scuri,⁴⁷ A. Sedov,⁴⁹ S. Seidel,³⁸ Y. Seiya,⁴² A. Semenov,¹⁶ L. Sexton-Kennedy,¹⁸ F. Sforza^{ee},⁴⁷ A. Sfyrla,²⁵ S.Z. Shalhout,⁵⁹ T. Shears,³⁰ P.F. Shepard,⁴⁸ M. Shimojima^t,⁵⁶ S. Shiraiishi,¹⁴ M. Shochet,¹⁴ Y. Shon,⁶⁰ I. Shreyber,³⁷ A. Simonenko,¹⁶ P. Sinervo,³⁴ A. Sisakyan,¹⁶ A.J. Slaughter,¹⁸ J. Slaunwhite,⁴⁰ K. Sliwa,⁵⁷ J.R. Smith,⁸ F.D. Snider,¹⁸ R. Snihur,³⁴ A. Soha,¹⁸ S. Somalwar,⁵³ V. Sorin,⁴ P. Squillacioti^{ff},⁴⁷ M. Stanitzki,⁶¹ R. St. Denis,²² B. Stelzer,³⁴ O. Stelzer-Chilton,³⁴ D. Stentz,³⁹ J. Strologas,³⁸ G.L. Strycker,³⁵ J.S. Suh,²⁸ A. Sukhanov,¹⁹ I. Suslov,¹⁶ A. Taffard^f,²⁵ R. Takashima,⁴¹ Y. Takeuchi,⁵⁶ R. Tanaka,⁴¹ J. Tang,¹⁴ M. Tecchio,³⁵ P.K. Teng,¹ J. Thom^h,¹⁸ J. Thome,¹³ G.A. Thompson,²⁵ E. Thomson,⁴⁶ P. Tipton,⁶¹ P. Tito-Guzmán,³² S. Tkaczyk,¹⁸ D. Toback,⁵⁴ S. Tokar,¹⁵ K. Tollefson,³⁶ T. Tomura,⁵⁶ D. Tonelli,¹⁸ S. Torre,²⁰ D. Torretta,¹⁸ P. Totaroⁱⁱ,⁵⁵ S. Tourneur,⁴⁵ M. Trovato^{gg},⁴⁷ S.-Y. Tsai,¹ Y. Tu,⁴⁶ N. Turini^{ff},⁴⁷ F. Ukegawa,⁵⁶ S. Uozumi,²⁸ N. van Remortel^b,²⁴ A. Varganov,³⁵ E. Vataga^{gg},⁴⁷ F. Vázquezⁿ,¹⁹ G. Velev,¹⁸ C. Vellidis,³ M. Vidal,³² I. Vila,¹² R. Vilar,¹² M. Vogel,³⁸ I. Volobouev^w,²⁹ G. Volpi^{ee},⁴⁷ P. Wagner,⁴⁶ R.G. Wagner,² R.L. Wagner,¹⁸ W. Wagner^{aa},²⁷ J. Wagner-Kuhr,²⁷ T. Wakisaka,⁴² R. Wallny,⁹ S.M. Wang,¹ A. Warburton,³⁴ D. Waters,³¹ M. Weinberger,⁵⁴ J. Weinelt,²⁷ W.C. Wester III,¹⁸ B. Whitehouse,⁵⁷ D. Whiteson^f,⁴⁶ A.B. Wicklund,² E. Wicklund,¹⁸ S. Wilbur,¹⁴ G. Williams,³⁴ H.H. Williams,⁴⁶ P. Wilson,¹⁸ B.L. Winer,⁴⁰ P. Wittich^h,¹⁸ S. Wolbers,¹⁸ C. Wolfe,¹⁴ H. Wolfe,⁴⁰ T. Wright,³⁵ X. Wu,²¹ F. Würthwein,¹⁰ A. Yagil,¹⁰ K. Yamamoto,⁴² J. Yamaoka,¹⁷ U.K. Yang^r,¹⁴ Y.C. Yang,²⁸ W.M. Yao,²⁹ G.P. Yeh,¹⁸ K. Yi^o,¹⁸ J. Yoh,¹⁸ K. Yorita,⁵⁸ T. Yoshida^l,⁴² G.B. Yu,¹⁷ I. Yu,²⁸ S.S. Yu,¹⁸ J.C. Yun,¹⁸ A. Zanetti,⁵⁵ Y. Zeng,¹⁷ X. Zhang,²⁵ Y. Zheng^d,⁹ and S. Zucchelli^{cc}⁶

(CDF Collaboration[†])

¹Institute of Physics, Academia Sinica, Taipei, Taiwan 11529, Republic of China

²Argonne National Laboratory, Argonne, Illinois 60439

³University of Athens, 157 71 Athens, Greece

⁴Institut de Fisica d'Altes Energies, Universitat Autònoma de Barcelona, E-08193, Bellaterra (Barcelona), Spain

⁵Baylor University, Waco, Texas 76798

⁶Istituto Nazionale di Fisica Nucleare Bologna, ^{cc}University of Bologna, I-40127 Bologna, Italy

⁷Brandeis University, Waltham, Massachusetts 02254

⁸University of California, Davis, Davis, California 95616

⁹University of California, Los Angeles, Los Angeles, California 90024

¹⁰University of California, San Diego, La Jolla, California 92093

¹¹University of California, Santa Barbara, Santa Barbara, California 93106

¹²Instituto de Fisica de Cantabria, CSIC-University of Cantabria, 39005 Santander, Spain

¹³Carnegie Mellon University, Pittsburgh, PA 15213

¹⁴Enrico Fermi Institute, University of Chicago, Chicago, Illinois 60637

¹⁵Comenius University, 842 48 Bratislava, Slovakia; Institute of Experimental Physics, 040 01 Kosice, Slovakia

¹⁶Joint Institute for Nuclear Research, RU-141980 Dubna, Russia

¹⁷Duke University, Durham, North Carolina 27708

¹⁸Fermi National Accelerator Laboratory, Batavia, Illinois 60510

¹⁹University of Florida, Gainesville, Florida 32611

²⁰Laboratori Nazionali di Frascati, Istituto Nazionale di Fisica Nucleare, I-00044 Frascati, Italy

²¹University of Geneva, CH-1211 Geneva 4, Switzerland

²²Glasgow University, Glasgow G12 8QQ, United Kingdom

²³Harvard University, Cambridge, Massachusetts 02138

²⁴Division of High Energy Physics, Department of Physics,

University of Helsinki and Helsinki Institute of Physics, FIN-00014, Helsinki, Finland

²⁵University of Illinois, Urbana, Illinois 61801

²⁶The Johns Hopkins University, Baltimore, Maryland 21218

- ²⁷Institut für Experimentelle Kernphysik, Karlsruhe Institute of Technology, D-76131 Karlsruhe, Germany
²⁸Center for High Energy Physics: Kyungpook National University,
Daequ 702-701, Korea; Seoul National University, Seoul 151-742,
Korea; Sungkyunkwan University, Suwon 440-746,
Korea; Korea Institute of Science and Technology Information,
Daejeon 305-806, Korea; Chonnam National University, Gwangju 500-757,
Korea; Chonbuk National University, Jeonju 561-756, Korea
²⁹Ernest Orlando Lawrence Berkeley National Laboratory, Berkeley, California 94720
³⁰University of Liverpool, Liverpool L69 7ZE, United Kingdom
³¹University College London, London WC1E 6BT, United Kingdom
³²Centro de Investigaciones Energeticas Medioambientales y Tecnologicas, E-28040 Madrid, Spain
³³Massachusetts Institute of Technology, Cambridge, Massachusetts 02139
³⁴Institute of Particle Physics: McGill University, Montréal, Québec,
Canada H3A 2T8; Simon Fraser University, Burnaby, British Columbia,
Canada V5A 1S6; University of Toronto, Toronto, Ontario,
Canada M5S 1A7; and TRIUMF, Vancouver, British Columbia, Canada V6T 2A3
³⁵University of Michigan, Ann Arbor, Michigan 48109
³⁶Michigan State University, East Lansing, Michigan 48824
³⁷Institution for Theoretical and Experimental Physics, ITEP, Moscow 117259, Russia
³⁸University of New Mexico, Albuquerque, New Mexico 87131
³⁹Northwestern University, Evanston, Illinois 60208
⁴⁰The Ohio State University, Columbus, Ohio 43210
⁴¹Okayama University, Okayama 700-8530, Japan
⁴²Osaka City University, Osaka 588, Japan
⁴³University of Oxford, Oxford OX1 3RH, United Kingdom
⁴⁴Istituto Nazionale di Fisica Nucleare, Sezione di Padova-Trento, ^{dd}University of Padova, I-35131 Padova, Italy
⁴⁵LPNHE, Université Pierre et Marie Curie/IN2P3-CNRS, UMR7585, Paris, F-75252 France
⁴⁶University of Pennsylvania, Philadelphia, Pennsylvania 19104
⁴⁷Istituto Nazionale di Fisica Nucleare Pisa, ^{ee}University of Pisa,
^{ff}University of Siena and ^{gg}Scuola Normale Superiore, I-56127 Pisa, Italy
⁴⁸University of Pittsburgh, Pittsburgh, Pennsylvania 15260
⁴⁹Purdue University, West Lafayette, Indiana 47907
⁵⁰University of Rochester, Rochester, New York 14627
⁵¹The Rockefeller University, New York, New York 10021
⁵²Istituto Nazionale di Fisica Nucleare, Sezione di Roma 1,
^{hh}Sapienza Università di Roma, I-00185 Roma, Italy
⁵³Rutgers University, Piscataway, New Jersey 08855
⁵⁴Texas A&M University, College Station, Texas 77843
⁵⁵Istituto Nazionale di Fisica Nucleare Trieste/Udine,
I-34100 Trieste, ⁱⁱUniversity of Trieste/Udine, I-33100 Udine, Italy
⁵⁶University of Tsukuba, Tsukuba, Ibaraki 305, Japan
⁵⁷Tufts University, Medford, Massachusetts 02155
⁵⁸Waseda University, Tokyo 169, Japan
⁵⁹Wayne State University, Detroit, Michigan 48201
⁶⁰University of Wisconsin, Madison, Wisconsin 53706
⁶¹Yale University, New Haven, Connecticut 06520

We report two complementary measurements of the diboson ($WW + WZ$) cross section in the final state consisting of an electron or muon, missing transverse energy, and jets, performed using $p\bar{p}$ collision data at $\sqrt{s} = 1.96$ TeV collected by the Collider Detector at Fermilab. The first method uses the dijet invariant mass distribution while the second method uses more of the kinematic information in the event through matrix-element calculations of the signal and background processes and has a higher sensitivity. The result from the second method has a signal significance of 5.4σ and is the first observation of $WW + WZ$ production using this signature. Combining the results from both methods gives $\sigma_{WW+WZ} = 16.0 \pm 3.3$ pb, in agreement with the standard model prediction.

PACS numbers: 14.80.Bn, 14.70.Fm, 14.70.Hp, 12.15.Ji

*Deceased

[†]With visitors from ^aUniversity of Massachusetts Amherst,

Amherst, Massachusetts 01003, ^bUniversiteit Antwerpen, B-2610

Measurements involving heavy vector boson pairs (WW , WZ , and ZZ) are important tests of the electroweak sector of the standard model (SM). Deviations of the production cross section from predictions could arise from anomalous triple gauge boson interactions [1] or from new resonances decaying to vector bosons. Furthermore, the topology of diboson events is similar to that of events in which a Higgs boson is produced in association with a W or a Z , allowing diboson measurements to provide an important step towards future measurements of Higgs boson production.

Diboson production has been observed at the Tevatron in channels in which both bosons decay leptonically [2, 3]. Extraction of the diboson signal in hadronic channels is more challenging because of significantly larger backgrounds. In addition, due to limited detector resolution, it is difficult to distinguish hadronically decaying W bosons from Z bosons. We report on two measurements of the cross section, $\sigma(p\bar{p} \rightarrow WW + WZ)$, that use different techniques applied to the leptonic decay of one W and the hadronic decay of the associated W or Z ($WW/WZ \rightarrow \ell\nu qq$, where ℓ represents an electron or muon). Our result represents the first observation of this signal in the lepton + jets channel. Evidence has previously been reported by the D0 collaboration [4], and the CDF collaboration set a limit on its cross section times branching ratio [5]. In addition the CDF collaboration has reported observation of $WW + WZ + ZZ$ in a different hadronic channel with large missing transverse energy and jets [6].

The first method uses the invariant mass of the two-jet system (M_{jj}) to extract a signal peak from data corresponding to 3.9 fb^{-1} of $p\bar{p}$ collisions at $\sqrt{s} = 1.96 \text{ TeV}$.

The second method takes advantage of more kinematic information in the event by constructing a discriminant based on calculations of the differential cross sections of the signal and background processes. This so-called matrix-element (ME) method has been employed in a search for a low-mass Higgs produced in association with a W boson [7] and in a measurement of single top production [8]. It is expected to achieve greater discriminating power and here uses data corresponding to an integrated luminosity of 2.7 fb^{-1} .

The aspects of the CDF II detector [9] relevant to these analyses are briefly described here. The tracking system is composed of silicon microstrip detectors and an open-cell drift chamber inside a 1.4 T solenoid. Electromagnetic lead-scintillator and hadronic iron-scintillator sampling calorimeters segmented in a projective geometry surround the tracking detectors. A central calorimeter covers a pseudorapidity range of $|\eta| < 1.1$ while plug calorimeters extend the acceptance into the region $1.1 < |\eta| < 3.6$. Outside of the calorimeters are muon detectors composed of scintillators and drift chambers. Cherenkov counters around the beam pipe and in the plug calorimeters count the inelastic collisions per bunch crossing and provide the luminosity measurement.

Data samples common to both analyses use trigger selections requiring a central electron (muon) with $E_T (p_T) > 18 \text{ GeV}$. The ME method utilizes an additional sample derived from a trigger requiring two jets and large missing transverse energy (\cancel{E}_T) [10].

Offline we select events with electron (muon) candidates with $E_T (p_T) > 20 \text{ GeV}$, and with \cancel{E}_T , jet, and other kinematic requirements chosen differently for the two methods. Jets are clustered using a fixed-cone algorithm with radius $\Delta R = \sqrt{(\Delta\eta)^2 + (\Delta\phi)^2} = 0.4$ and their energies are corrected for detector effects [11]. Cosmic ray and photon conversion candidates are identified and removed.

Further event selection requirements are made to reduce backgrounds and the sensitivity to systematic uncertainties. In the M_{jj} method, we require events to have $\cancel{E}_T > 25 \text{ GeV}$, at least two jets with $E_T > 15 \text{ GeV}$ and $|\eta| < 2.4$, and the dijet vector boson candidate to have $p_T > 40 \text{ GeV}/c$. As a result of these selection criteria, the M_{jj} distribution for background is smoothly falling in the region where the signal is expected to peak. The invariant mass of the dijet vector boson candidate, M_{jj} , is evaluated from the two most energetic jets. Additional requirements are made to reduce backgrounds and improve the Monte Carlo modeling of event kinematics: the transverse mass of the lepton and \cancel{E}_T system ($M_T(W)$ [10]) must be greater than $30 \text{ GeV}/c^2$, and the two most energetic jets must be separated by $|\Delta\eta| < 2.5$.

In the ME method, we require events to have $\cancel{E}_T > 20 \text{ GeV}$ and exactly two jets with $E_T > 25 \text{ GeV}$ and $|\eta| < 2.0$. Additional selection criteria to reduce backgrounds and achieve good modeling of the quantities used

Antwerp, Belgium, ^cUniversity of Bristol, Bristol BS8 1TL, United Kingdom, ^dChinese Academy of Sciences, Beijing 100864, China, ^eIstituto Nazionale di Fisica Nucleare, Sezione di Cagliari, 09042 Monserrato (Cagliari), Italy, ^fUniversity of California Irvine, Irvine, CA 92697, ^gUniversity of California Santa Cruz, Santa Cruz, CA 95064, ^hCornell University, Ithaca, NY 14853, ⁱUniversity of Cyprus, Nicosia CY-1678, Cyprus, ^jUniversity College Dublin, Dublin 4, Ireland, ^kUniversity of Edinburgh, Edinburgh EH9 3JZ, United Kingdom, ^lUniversity of Fukui, Fukui City, Fukui Prefecture, Japan 910-0017 ^mKinki University, Higashiosaka City, Japan 577-8502 ⁿUniversidad Iberoamericana, Mexico D.F., Mexico, ^oUniversity of Iowa, Iowa City, IA 52242, ^pKansas State University, Manhattan, KS 66506 ^qQueen Mary, University of London, London, E1 4NS, England, ^rUniversity of Manchester, Manchester M13 9PL, England, ^sMuons, Inc., Batavia, IL 60510, ^tNagasaki Institute of Applied Science, Nagasaki, Japan, ^uUniversity of Notre Dame, Notre Dame, IN 46556, ^vUniversity de Oviedo, E-33007 Oviedo, Spain, ^wTexas Tech University, Lubbock, TX 79409, ^xIFIC(CSIC-Universitat de Valencia), 56071 Valencia, Spain, ^yUniversidad Tecnica Federico Santa Maria, 110v Valparaiso, Chile, ^zUniversity of Virginia, Charlottesville, VA 22906 ^{aa}Bergische Universitat Wuppertal, 42097 Wuppertal, Germany, ^{bb}Yarmouk University, Irbid 211-63, Jordan ^{jj}On leave from J. Stefan Institute, Ljubljana, Slovenia,

in the matrix element calculation include the rejection of events with either an additional jet of $E_T > 12$ GeV or a second charged lepton. The latter reduces $Z+jets$, $t\bar{t}$, and leptonic diboson backgrounds. For events with an electron candidate, there is a significant background from production of multiple jets (multi-jet in the following) by quantum chromodynamical (QCD) processes, where the electron is faked by a hadronic jet. The ME method deals with this background by applying stringent selection criteria, while the M_{jj} method assigns a systematic uncertainty to the background shape. The reduction of the multi-jet QCD background in the ME analysis is achieved by raising the \cancel{E}_T cut to 40 GeV, requiring $M_T(W) > 70$ GeV/ c^2 , and imposing additional cuts on the angles between the jets, the lepton, and the \cancel{E}_T [12]. There is a less stringent requirement of $M_T(W) > 10$ GeV/ c^2 imposed on muon events to reduce the QCD background in that channel.

After these selections for both methods, the dominant background to the diboson signal is a W boson produced with accompanying jets ($W+jets$), where the W decays leptonically. Smaller but non-negligible backgrounds come from QCD multi-jet (where one jet mimics a lepton signature), $Z+jets$, $t\bar{t}$, and single top production. QCD multi-jet events are modeled using data with loosened lepton selection criteria. All other signal and background processes are modeled using event generators and a GEANT-based CDF II detector simulation. The diboson signals as well as the $t\bar{t}$ and single top backgrounds are simulated using the PYTHIA event generator [14]. The $W+jets$ and $Z+jets$ backgrounds are simulated using the tree-level event generator ALPGEN [15], with an interface to PYTHIA providing parton showering and hadronization.

The normalization of the $Z+jets$ background is based on the measured cross section while for $t\bar{t}$ and single top backgrounds the NLO predicted cross section is used [16]. The efficiencies for the $Z+jets$, $t\bar{t}$, and single top backgrounds are estimated from simulation. The normalization of the QCD background is estimated by fitting the \cancel{E}_T spectrum in data to the sum of all contributing processes, where the QCD and $W+jets$ normalizations float in the fit. In the final signal extractions from both methods, the multi-jet QCD background is Gaussian constrained to the result of this \cancel{E}_T fit and the $W+jets$ background is left unconstrained.

We now describe the methodology and results from each technique. In the M_{jj} method we extract the signal fraction from the data by performing a χ^2 fit to the dijet invariant mass spectrum, separately for electron and muon events. Templates of M_{jj} distributions are constructed with the multi-jet QCD background, the signal $WW + WZ$ processes, and the sum of the electroweak backgrounds ($Z + jets$, $W + jets$, and $t\bar{t}$ production).

Figure 1 shows the fit results superimposed on data after the electron and muon samples are combined. Also

shown is the data M_{jj} distribution after having subtracted the estimated background, superimposed on the signal Monte Carlo shape extracted from the fit. Combining the two χ^2 fit results we get a total of $1079 \pm 232(\text{stat}) \pm 86(\text{syst})$ $WW/WZ \rightarrow \ell\nu jj$ events, of which about 60% are muon events and 40% are electron events. The observed significance is 4.6σ where 4.9σ is expected, which is obtained by combining the separate results from the electron and muon channels. The resultant $WW + WZ$ production cross section measurement is $\sigma_{WW+WZ} = 14.4 \pm 3.1(\text{stat}) \pm 2.2(\text{syst})$ pb. The sources of systematic uncertainty in this measurement are discussed together with those from the ME method below.

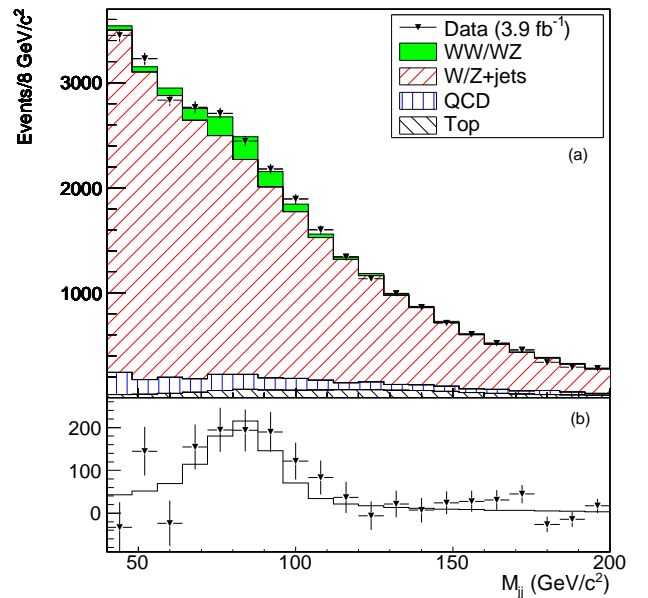


FIG. 1: Dijet invariant mass distribution of reconstructed $W/Z \rightarrow jj$ candidates compared to the fitted signal and background components (a), and for the corresponding background subtracted distribution (b).

TABLE I: Expected and observed event yields after the ME method selection in 2.7 fb^{-1} of data.

Process	Predicted event yield
WW signal	446 ± 29
WZ signal	79 ± 6
$W+jets$	10175 ± 305
$Z+jets$	584 ± 88
QCD multi-jet	283 ± 113
$t\bar{t} + \text{single top}$	241 ± 29
Observed	11812

In the ME method a probability density $P(x)$ that an event was produced by a given process is determined using the standard model differential cross section for that

process. For an event with measured quantities x , we integrate the appropriate differential cross section $d\sigma(y)$ over the partonic quantities y convolved with the parton distribution functions (PDFs), $f(y_1), f(y_2)$, and over transfer functions describing detector resolution effects, $W(y, x)$:

$$P(x) = \frac{1}{\sigma} \int d\sigma(y) dq_1 dq_2 f(y_1) f(y_2) W(y, x). \quad (1)$$

We use the CTEQ5L PDF parameterization [17]. $W(x, y)$ is a mapping of measured jet energy to partonic energy derived using the full detector simulation, while the lepton momenta and jet angles are assumed to be measured exactly. The integration is performed over the energy of the partons and the longitudinal momentum of the neutrino. The matrix element is calculated with tree-level diagrams from MADGRAPH [18]. Event probability densities P_x are calculated for the signal processes WW and WZ , as well as for W plus two parton and single top background processes. The event probabilities are combined into an event probability discriminant: $EPD = P_{signal}/(P_{signal} + P_{background})$, where $P_{signal} = P_{WW} + P_{WZ}$ and $P_{background} = P_{W+jets} + P_{single\ top}$. We make templates of the EPD for all signal and background processes and ultimately extract the signal using a fit of the observed EPD distribution to a sum of the signal and background templates. The expected event yields are as shown in Table I for the ME method's event selection.

Figure 2 shows the dijet mass in bins of EPD . Most of the background events have low EPD . Events with $EPD > 0.25$ have a dijet mass peak close to the expected W/Z resonance, and the signal-to-background ratio improves with increasing EPD .

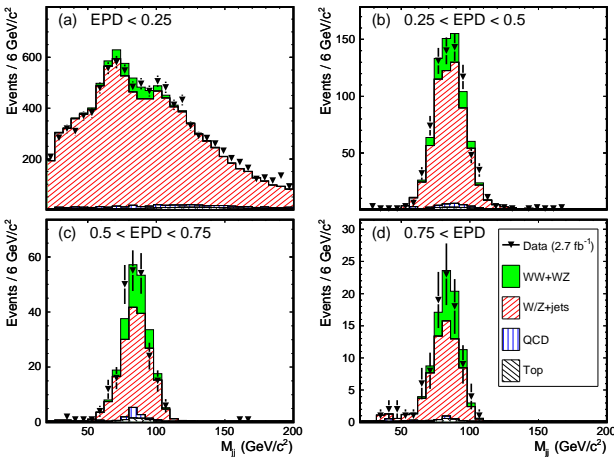


FIG. 2: M_{jj} for events with (a) $EPD < 0.25$, (b) $0.25 < EPD < 0.5$, (c) $0.5 < EPD < 0.75$, and (d) $EPD > 0.75$.

Before comparing the observed EPD to the prediction, we validate the Monte Carlo modeling of the quantities

that enter the matrix element calculation. We compare the observed distributions to the predicted ones in control regions with very little signal and also in the signal-rich region. The different regions are chosen according to the invariant mass of the two-jet system (M_{jj}): the signal-rich region has $55 < M_{jj} < 120$ GeV and the control regions cover the rest of the M_{jj} range. We also check the modeling of the properties (mass, p_T , and η) of the leptonic W boson and the hadronic W or Z boson candidate. All of these quantities are well described by the simulation for our event selection. There is a small discrepancy in the description of M_{jj} in the control regions, as is visible in the low- EPD region of Figure 2. Associated with this discrepancy we assign a systematic mismodeling uncertainty which is derived in the control regions and extrapolated through the signal region. This uncertainty has a negligible effect on the results, because most background events lie in the first few bins of the EPD distribution. Small changes in modeling of those background events do not change the shape of the EPD .

The observed and predicted $EPDs$ are shown in Figure 3. We use a binned-likelihood fit of the observed EPD to a sum of templates, testing both a background-only hypothesis and a signal-plus-background ($s+b$) hypothesis. Systematic uncertainties, discussed further below, are included in the fit as constrained parameters. We perform pseudo experiments to calculate the probability (p -value) that the background-only discriminant fluctuates up to the observed result (observed p -value) and up to the median expected $s+b$ result (expected p -value). We observe a p -value of 2.1×10^{-7} , corresponding to a signal significance of 5.4σ , where 5.1σ is expected. The observed $WW + WZ$ cross section is $\sigma_{WW+WZ} = 17.7 \pm 3.1(\text{stat}) \pm 2.4(\text{syst}) \text{ pb}$.

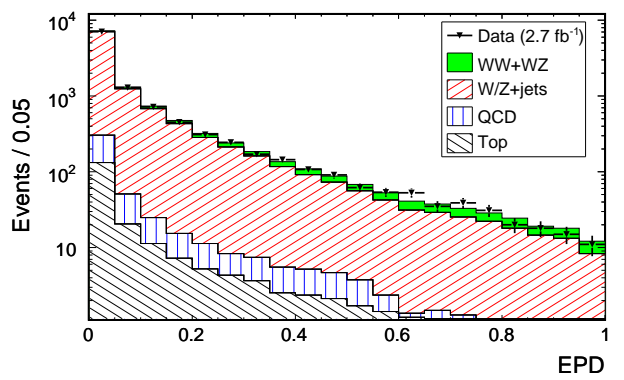


FIG. 3: Observed EPD distribution superimposed on distribution expected from simulated processes.

We consider several sources of systematic uncertainty in both methods, taking into account their effect on both the signal acceptance and the shape of the background and signal templates. The uncertainty on the normaliza-

tion of the backgrounds is taken as part of the statistical uncertainty. In the M_{jj} method the largest systematic uncertainties are due to the modeling of the electroweak and QCD shapes, about 8% and 6% respectively. In the ME method the uncertainty in the jet energy scale is the largest systematic uncertainty, at about 10%, which includes contributions both from the signal acceptance and from the shapes of the signal templates. In the M_{jj} method this uncertainty is about 6%. Both methods include an uncertainty of about 5% due to initial and final state radiation and a 6% uncertainty on the integrated luminosity. Smaller contributions arise from PDFs, jet energy resolution, the factorization and renormalization scales used in the $W+jets$ simulation, and trigger and lepton identification efficiencies.

One measure of how the two methods are correlated is the expected overlap of $WW + WZ$ signal. Accounting for the different integrated luminosities used, 15% of the signal in the M_{jj} analysis is common to that in the *EPD* analysis. Conversely, 29% of the signal in the *EPD* analysis is common to that in the M_{jj} analysis. This corresponds to a statistical correlation of about 21%. If we assume the systematic uncertainties are 100% correlated, then the total correlation between the two analyses is 49%, leading to a combined [19] result of $\sigma_{WW+WZ} = 16.0 \pm 3.3(\text{stat+syst}) \text{ pb}$. Because the total uncertainties on the two input measurements are so similar, the combined central value does not depend significantly on the correlation assumed. The total uncertainty in the combined result increases with increasing correlation and we quote the value assuming maximum possible correlation. The signal overlap with the CDF $WW + WZ + ZZ$ observation in the $\cancel{E}_T + \text{jets}$ channel [6] is also studied. While that analysis requires much larger \cancel{E}_T , it does not veto events with identified leptons. We found that about 15% of the $WW + WZ$ signal from the $\cancel{E}_T + \text{jets}$ analysis appears in the analyses presented here.

In summary, we observe $WW + WZ$ production in the lepton plus jets plus \cancel{E}_T final state. We perform two searches: one seeking a resonance on top of a smoothly falling dijet mass distribution, and another building a discriminant using a matrix element technique. The combined $WW + WZ$ cross section from these two methods is measured to be $\sigma_{WW+WZ} = 16.0 \pm 3.3(\text{stat+syst}) \text{ pb}$, in good agreement with the SM prediction of $16.1 \pm 0.9 \text{ pb}$ [20]. Measurements of these diboson processes are a necessary step toward validating Higgs boson search techniques at the Tevatron.

We thank the Fermilab staff and the technical staffs of the participating institutions for their vital contributions. This work was supported by the U.S. Department of Energy and National Science Foundation; the Italian Istituto Nazionale di Fisica Nucleare; the Ministry of Education, Culture, Sports, Science and Technology of Japan; the Natural Sciences and Engineering Research Council of Canada; the National Science Council of the

Republic of China; the Swiss National Science Foundation; the A.P. Sloan Foundation; the Bundesministerium für Bildung und Forschung, Germany; the World Class University Program, the National Research Foundation of Korea; the Science and Technology Facilities Council and the Royal Society, UK; the Institut National de Physique Nucléaire et Physique des Particules/CNRS; the Russian Foundation for Basic Research; the Ministerio de Ciencia e Innovación, and Programa Consolider-Ingenio 2010, Spain; the Slovak R&D Agency; and the Academy of Finland.

-
- [1] K. Hagiwara, S. Ishihara, R. Szalapski, and D. Zeppenfeld, Phys. Rev. D **48**, 2182 (1993).
 - [2] D. Acosta *et al.* (CDF Collaboration), Phys. Rev. Lett. **94**, 211801 (2005); A. Abulencia *et al.* (CDF Collaboration), *ibid* **98**, 161801 (2007); T. Aaltonen *et al.* (CDF Collaboration), *ibid* **100**, 201801 (2008).
 - [3] V.M. Abazov *et al.* (D0 Collaboration), Phys. Rev. Lett. **94**, 151801 (2005) and Phys. Rev. D **76**, 111104(R) (2007).
 - [4] V. M. Abazov *et al.* (DO collaboration), Phys. Rev. Lett. **102**, 161801 (2009).
 - [5] T. Aaltonen *et al.* (CDF Collaboration), Phys. Rev. D **79**, 112011 (2009).
 - [6] T. Aaltonen *et al.* (CDF Collaboration), Phys. Rev. Lett. **103**, 091803 (2009).
 - [7] T. Aaltonen *et al.* (CDF Collaboration), Phys. Rev. Lett. **103**, 101802 (2009).
 - [8] T. Aaltonen *et al.* (CDF Collaboration), Phys. Rev. Lett. **101**, 252001 (2008); T. Aaltonen *et al.* (CDF Collaboration), Phys. Rev. Lett. **103**, 092002 (2009).
 - [9] D. Acosta *et al.* (CDF Collaboration), Phys. Rev. D **71**, 032001 (2005).
 - [10] We use a cylindrical coordinate system with its origin in the center of the detector, where θ and ϕ are the polar and azimuthal angles, respectively, and pseudorapidity is $\eta = -\ln \tan(\theta/2)$. The missing E_T (\vec{E}_T) is defined by $\vec{E}_T = -\sum_i E_T^i \hat{n}_i$, where \hat{n}_i is a unit vector perpendicular to the beam axis and pointing at the i^{th} calorimeter tower. \vec{E}_T is corrected for high-energy muons and also jet energy corrections. We define $\cancel{E}_T = |\vec{E}_T|$. The transverse momentum p_T is defined to be $p \sin \theta$. The transverse mass of the W is defined as $M_T(W) = \sqrt{2p_T^l \cancel{E}_T (1 - \cos(\Delta\Phi^{l\nu}))}$.
 - [11] A. Bhatti *et al.*, Nucl. Instrum. Methods A **566**, 375 (2006).
 - [12] P. Dong, Ph.D. thesis, University of California, Los Angeles, FERMILAB-THESIS-2008-12 (2008).
 - [13] J. Alwall *et al.*, J. High Energy Phys. 09 (2007) 028.
 - [14] T. Sjöstrand *et al.*, Comput. Phys. Commun., **135**, 238 (2001).
 - [15] M. L. Mangano *et al.*, J. High Energy Phys. 07 (2003) 001.
 - [16] D. Acosta *et al.* (CDF collaboration), Phys. Rev. Lett. **94**, 091803 (2005); M. Cacciari *et al.*, J. High Energy Phys. 09 (2008) 127; B. W. Harris *et al.*, Phys. Rev. D **66**, 054024 (2002).

- [17] J. Pumplin *et al.*, J. High Energy Phys. 07 (2002) 012.
- [18] F. Maltoni and T. Stelzer, J. High Energy Phys. 02 (2003) 027.
- [19] L. Lyons, D. Gibaut, and P. Clifford, Nucl. Instrum. Methods A **270**, 110 (1988).
- [20] J. M. Campbell and R. K. Ellis, Phys. Rev. D **60**, 113006 (1999).